INTEGRATING LOW-COST MEMS ACCELEROMETER MINI-ARRAYS (MAMA) IN EARTHQUAKE EARLY WARNING SYSTEMS

Ran N. Nof, Angela I. Chung, Horst Rademacher and Richard M. Allen

Berkeley Seismology Lab - UC Berkeley

ran.nof@gmail.com

Berkeley UNIVERSITY OF CALIFORNIA

Berkeley Seismology Lab

Department of Earth & Planetary Science

S23A-2738

1. Background

Current operational Earthquake Early Warning Systems (EEWS) acquire data from networks of single seismic stations, and compute source parameters assuming earthquakes to be point sources. For large events, the point-source assumption leads to an underestimation of magnitude, and the use of a single station leads to large uncertainties in the locations of events outside the network.

We propose the use of mini-arrays to improve EEWS. Mini-arrays have the potential to:

(a) Estimate reliable hypo-central locations using beam-forming (FK-analysis) techniques.

(b) Characterize the rupture dimensions and account for finite-source effects, leading to more reliable estimates for large magnitude earthquakes.

Previously, the high price of multiple seismometers has made creating arrays cost-prohibitive. However, we propose setting up mini-arrays of new low-cost (<$150) seismometers with high-performance class-C MEMS accelerometers around conventional seismic stations.

The expected benefits of such an approach include decreasing alert times, improving real time shaking predictions and mitigating false alarms.

2. Would it work?

In order to test the validity of using array processing techniques with low-cost MEMS, we used recordings from the Quake-Catcher Network low-cost 14-bit MEMS accelerometer array , deployed in Christchurch after the M7.2 Darfield earthquake (Lawrence et al., 2014). We use small sub-arrays of sensors to demonstrate our approach.

YES!

Using 10 stations and 3 stations, with a mini-array dimension of roughly 1.7km by 2.2km and 230m by 270m, and an array-epicenter distances of 13km and 11km, for the M5.1 and M4.7, respectively (Figure 1), we obtained a back azimuth (BAZ) estimate within ±4° and ±10° of the observed BAZ for the M5.1 and M4.7 earthquakes, respectively. As can be seen in Figure 2, the BAZ is stable almost immediately upon the onset of the P-wave.

3. Can we do better?

Though the 14-bit QCN sensors are sufficient for the previous example of finding the back-azimuth of a M4.7 earthquake at 11km, the sensors are less capable of resolving smaller or more-distant earthquakes. In order to improve detections, we have developed a stand alone MAMA Node (Figure 3).

The MAMA PCB Module has been designed as an expansion board for a RaspberryPi (RPI - Figure 4). Figure 5 outlines the device workflow.

4. How low can we go?

We present here the initial results from the new instrument. We first run a shake table test using a Güralp 5TC accelerometer as a reference (Figure 6). We then place a MAMA device alongside a QCN 16-bit Onavi-B sensor, co-located with the standard Episensor at the UC Berkeley Byerly vault station (BK.BKS). The Probabilistic Power Spectral Densities (PPSD) (McNamara and Buland, 2004) are plotted in Figure 7, comparing PPSD with typical spectral response of near-field and far-field earthquakes (Clinton and Heaton, 2002) and NHNM (Peterson 1993). This plot suggests that the MAMA device is expected to detect near-field events with M≥3.5. Since we are not limited by 16-bit sensors, we anticipate the next version to have lower noise levels, and lower detection thresholds.

Testing the Theory

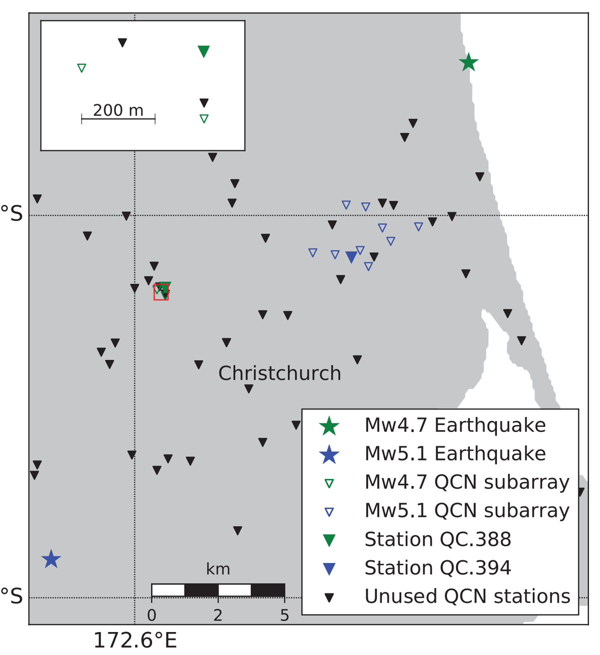

Figure 1: QCN Sub-arrays used for the BAZ solution are marked as blue and green triangles for Oct. 18, 2010, Mw 5.1 and Oct. 24, 2010 Mw 4.7 earthquakes (marked as stars in corresponding colors), respectively. Traces shown in Figure 2 are for stations marked as filled colored triangles (QC.388 and QC.394). Black triangles are QCN stations not used for the analysis. Not all QCN stations were available at all times. Inset location is marked as a red square.

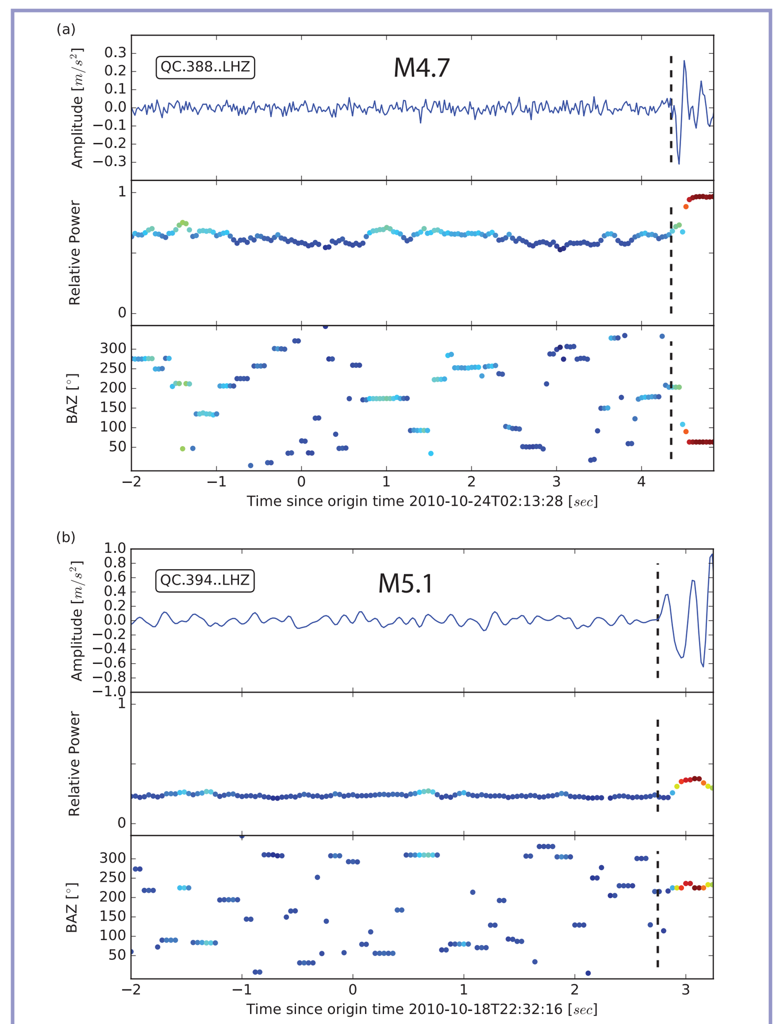

Figure 2: QCN BAZ calculation.
(a) The Mw4.7 event; (b) The Mw5.1 event. See Figure 1 for event locations. Each subplot shows:
Top - A vertical trace from a selected station, bandpass filtered at 1-8 Hz (blue line) and the P-wave arrival time (dashed dark line).
Middle - Maximum relative power of the FK-analysis (colored dots). Colors correspond to maximum (warm colors) and minimum (cold colors) values of the relative power in the plot.
Bottom - The corresponding BAZ. Colors correspond to relative-power values. X-axis origin is at the event origin time, showing data 2 seconds before origin time and 0.5 second after the P-wave onset at the representative station.

New MAMA Device

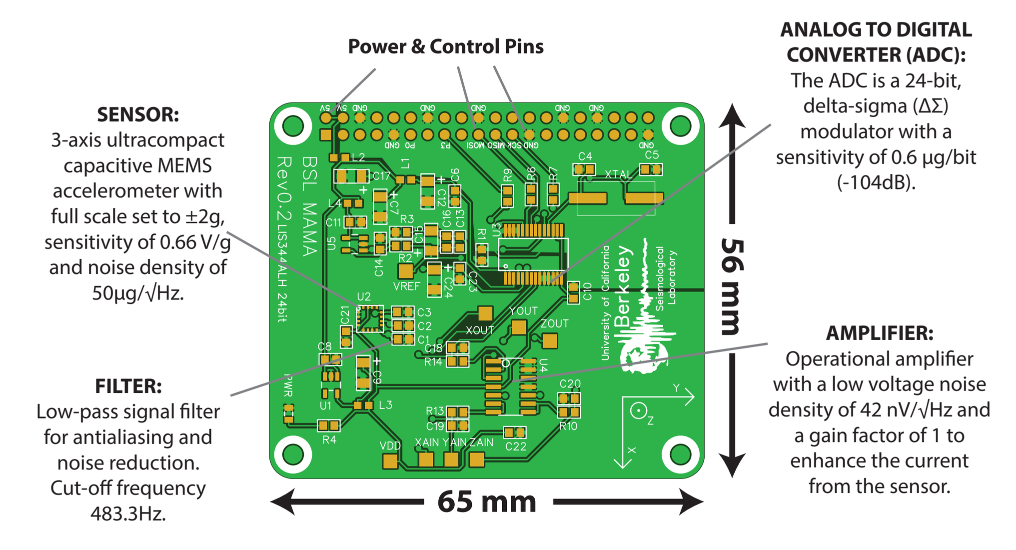

Figure 3: New MAMA PCB Module.

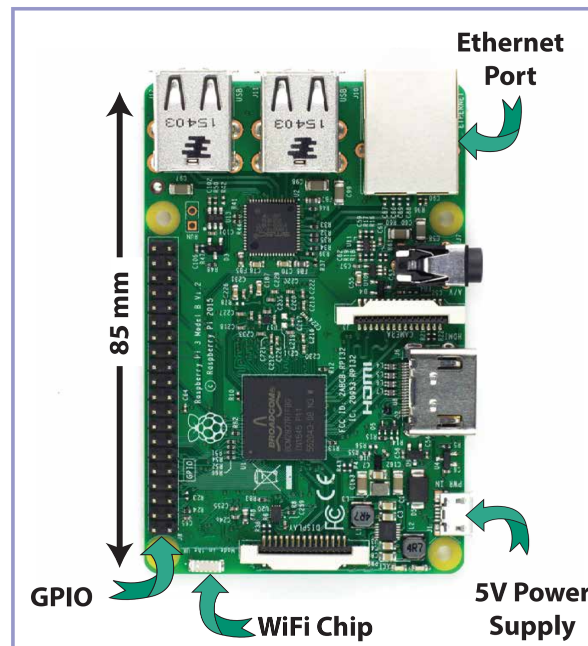

Figure 4: RaspberryPi 3B (RPI3) control unit for MAMA PCB.
The RPI3 is a single board computer equipped with a 1.2GHz 64-bit quad-core ARM8-A processor, 1GB RAM, Ethernet port and a WiFi chip. The RPI3 is connected to the MAMA PCB via the 40 GPIO pins, sampling the data and send it as miniseed packets through an onboard Seedlink server. The unit is powered by a 5V microUSB power supply.

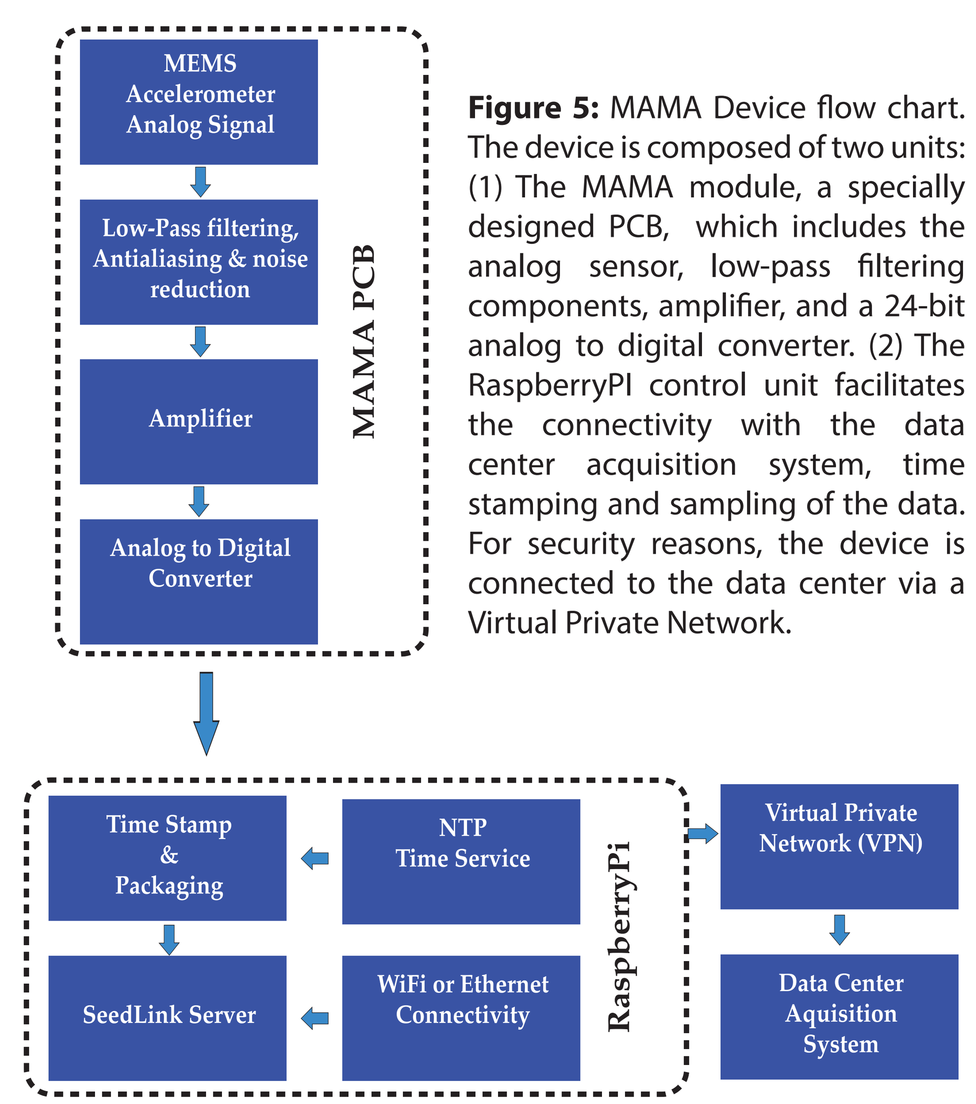

Figure 5: MAMA Device flow chart.
The device is composed of two units: (1) The MAMA module, a specially designed PCB, which includes the analog sensor, low-pass filtering components, amplifier, and a 24-bit analog to digital converter. (2) The RaspberryPI control unit facilitates the connectivity with the data center acquisition system, time stamping and sampling of the data. For security reasons, the device is connected to the data center via a Virtual Private Network.

Field Test Results

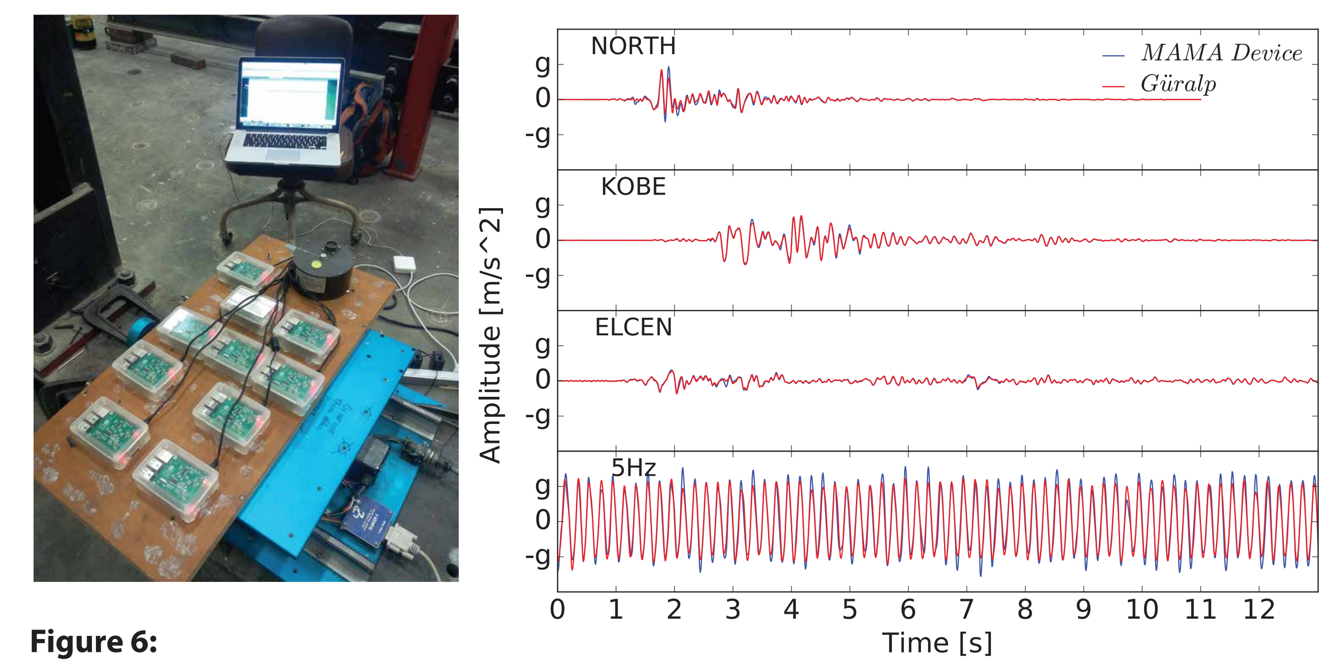

Figure 6:
Left: Shake-table test setting. The MAMA nodes are glued to a board that is screwed to the Quanser Shaker II shake-table. The Güralp 5TC accelerometer is also screwed to the board.
Right: Comparison between the 5TC accelerometer (red) and a representative trace from the MAMA nodes (blue) for selected tests. Traces are bandpass filtered between 0.5 Hz and 10 Hz.

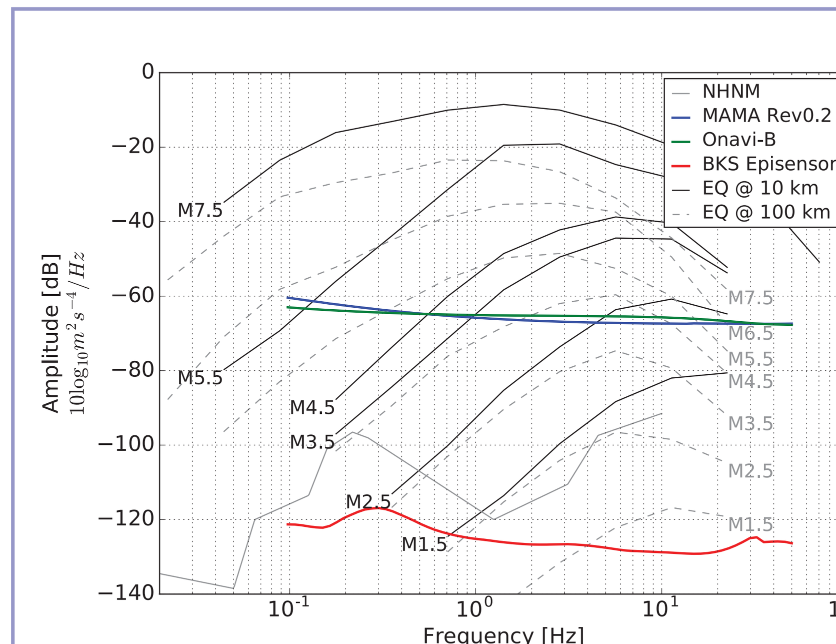

Figure 7: Comparison of mean horizontal trace PPSD of a MAMA node (blue), a QCN's ONAVI-B 16-bit MEMS sensor (green) and a conventional strong motion sensor of the BK network (red) installed at the Berkeley Byerly Vault, measured between 2016-09-01 and 2016-09-05.
Earthquake representative spectra response marked as dark solid and dashed gray lines for near and far fields, respectively. NHNM is marked as solid gray line.

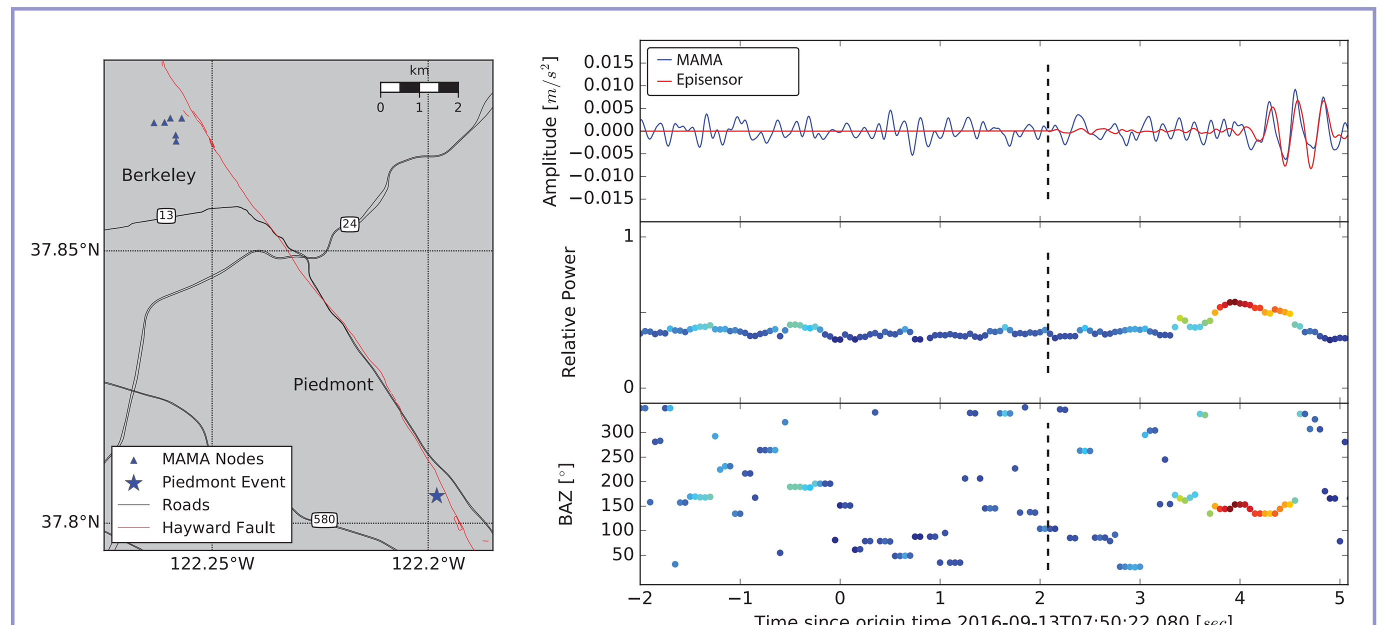

Figure 8:
Left: UC Berkeley campus MAMA location map (triangles) and the 2016-09-13 M3.5 Piedmont event (star). The Hayward fault is marked with a red line.
Right: MAMA BAZ calculation for the Mw3.5 2016-09-13 Piedmont event. Only MAMA nodes were used for this calculation. Top: Traces of BRK station Episensor and co-located MAMA device. See Figure 2 caption for more color and values explanation.

5. Field Test

We deployed six (6) MAMA nodes on the UC Berkeley campus around the seismic station (BK.BRK) in Havilland Hall. The maximum distance between two nodes of the MAMA is 600m. The M3.5 Piedmont event occurred on 2016-09-13 and was located ~9.5 km away (Figure 8, left). It was recorded by the MAMA nodes and analyzed as an example of MAMA performance in a realistic scenario. High levels of noise, particularly on the vertical channel, obscured the P-wave onset. The S-wave onset was detected by the MAMA nodes, and it was possible to calculate the BAZ for this event within 3 seconds of the P-wave arrival to the central conventional station BK.BRK (Figure 8, right). The observed BAZ is 144° and the calculated BAZ, where highest relative power values are observed, is 144°-153°.

6. Conclusions

As demonstrated, MAMA can be used to rapidly obtain the BAZ of an event. Combining multiple MAMA may make it possible to robustly estimate the epicenter of an earthquake based on just two station-arrays. This would decrease the time needed for point source EEWS to issue an alert. Implementing MAMA back-projection in real-time and incorporating that into EEWS will allow for the better estimation of earthquake magnitudes and shaking intensity distributions, based on finite-fault models rather than point-source models.

Acknowlegments

Ran Nof was funded by The Geological Survey of Israel (GSI), at the Ministry Energy and Water Resources. The authors would like to thank Oren Huber for his help with designing the PCB and to Sönke Möller for his help with assembling the first prototypes. Data was processed with ObsPy (Beyreuther et al., 2010). Figures were created with Matplotlib (Hunter, 2007).

References

Beyreuther, M., R. Barsch, L. Krischer, T. Megies, Y. Behr, and J. Wassermann. 2010. "ObsPy: A Python Toolbox for Seismology." Seismological Research Letters 81 (3): 530–33. doi:10.1785/gssrl.81.3.530.

Clinton, J. F., and T. H. Heaton. 2002. "Potential Advantages of a Strong-Motion Velocity Meter over a Strong-Motion Accelerometer." Seismological Research Letters 73 (3): 332–42. doi:10.1785/gssrl.73.3.332.

Hunter, John D. 2007. "Matplotlib: A 2D Graphics Environment." Computing in Science & Engineering 9 (3): 90–95. doi:10.1109/MCSE.2007.55.

Lawrence, J. F. et al. (2014), Rapid earthquake characterization using MEMS accelerometers and volunteer hosts following the M 7.2 Darfield, New Zealand, earthquake, Bull. Seismol. Soc. Am., 104(1), 184–192, doi:10.1785/0120120196.

McNamara, D. E. 2004. "Ambient Noise Levels in the Continental United States." Bulletin of the Seismological Society of America 94 (4): 1517–27. doi:10.1785/012003001.